

9

Resummation and hard thermal loops

We saw in the last chapter that QCD perturbation theory has problems at finite temperature, when taken into the infrared domain. These problems are the cause of the breakdown of the perturbative expansion of the pressure beyond $\mathcal{O}(g^6)$. We shall see here that these divergences are also responsible for the need to resum an infinite set of Feynman diagrams in order to compute a physical quantity at a given order in the coupling constant. These concepts were discussed before, in Chapter 3, when the set of ring diagrams was evaluated. In order to make the discussion as simple as possible, let us revisit the case of scalar $\lambda\phi^4$ theory.

Recalling our evaluation of the one-loop self-energy diagram, we had

$$\Pi_1 = 12\lambda T \sum_n \int \frac{d^3k}{(2\pi)^3} \frac{1}{\omega_n^2 + \omega^2} \quad (9.1)$$

As previously the vacuum contribution is renormalized by a mass counterterm and the complete self-energy, after analytic continuation to real energies, at finite temperature and at first order in the coupling is

$$\Pi_1^{\text{ren}} = 12\lambda \int \frac{d^3k}{(2\pi)^3} \frac{1}{\omega} \frac{1}{e^{\beta\omega} - 1} \quad (9.2)$$

In the high-temperature limit all masses are negligible, and then one can write $\Pi_1 \rightarrow \lambda T^2$. Therefore, at one-loop order thermal fluctuations generate a mass for the scalar field, $m_{\text{eff}} = \sqrt{\lambda}T$. Notice that in the massless limit the integral in (9.2) is dominated by momenta of the order of the temperature, $k \sim T$. In our high-temperature limit these momenta would be referred to as “hard”. The effects of the thermal mass can be incorporated by defining an effective propagator which, in frequency–momentum

space, would be given by

$$\mathcal{D}^*(\omega_n, \mathbf{k}) = \frac{1}{\omega_n^2 + \mathbf{k}^2 + \lambda T^2} \quad (9.3)$$

This simple example tells us that if momenta are of the order of the temperature, or hard, the self-energy correction to the propagator is a perturbative correction and can be neglected. However, if the momentum is “soft”, so that $k \sim \sqrt{\lambda}T$, then the thermal mass term is as large as the inverse bare propagator and certainly must be included. In this limit, the correction is as big as the leading term. The previous discussion also suggests that it is useful to define hard, $k \simeq T$, and soft, $k \simeq \sqrt{\lambda}T$, scales of momenta. Here k means indiscriminately energy or momentum. An instructive exercise consists of recalculating the self-energy, only this time using the effective propagator defined above. The only change from the previous evaluation of the self-energy is that now one has the energy appropriate for a massive field, $\omega = \sqrt{k^2 + m_{\text{eff}}^2}$. We examine the behavior of the integrand, which is largely dictated by the distribution function, and recall that $m_{\text{eff}}/T = \sqrt{\lambda}$. The contribution to the integral from hard momenta is small and generates corrections of order λ to the self-energy. The contribution to the integral from soft momenta allows the distribution function to be approximated by $N_B(\omega) \approx T/\omega$. Keeping in mind that the upper limit in this case is of order $\sqrt{\lambda}T$, we get a contribution to Π of order

$$\Pi \sim \frac{\lambda T}{m_{\text{eff}}^2} \int_0^{\sqrt{\lambda}T} dk k^2$$

The quantitative result is

$$m_*^2 = m_{\text{eff}}^2 \left(1 - \frac{3m_{\text{eff}}}{\pi T} + \dots \right) \quad (9.4)$$

The improved effective mass is the same as m_{eff} to leading order but also contains a correction of order $\sqrt{\lambda}$ which is given entirely by the soft momenta in the loop integral. Importantly, this correction is obtained if one uses the effective propagator (9.3), which represents a resummation of an infinite set of higher-order diagrams. It is instructive to note that even though each of these diagrams is infrared divergent, their sum is finite. We have encountered this situation previously in the form of the ring diagrams in Chapter 3.

The scalar field application is considerably simpler than that of gauge theories, but it conveys the essential part of the message: in order to calculate systematically amplitudes with soft lines, it is necessary to resum perturbation theory by including all possible hard thermal loops. We shall see that, in general, this procedure involves effective propagators

and vertices. In $\lambda\phi^4$ theory, it is sufficient to consider only the effective propagator as defined above. Since the coupling depends on the temperature only logarithmically, the use of bare vertices is adequate. The case of gauge theories is more involved technically because the self-energy is generally energy and momentum dependent, and because there are vertices that are energy and momentum dependent. Also, there is a rich set of important physical scales in weakly coupled gauge theories. The next section outlines how to pick out the contributions of hard thermal loops from a diagram with soft external four-momenta.

9.1 Isolating the hard thermal loop contribution

We will concentrate here on one-loop diagrams and generalize later. We follow the original treatment of Pisarski and Braaten [1, 2]. As discussed previously, the evaluation of one-loop self-energies involves a sum over discrete frequencies as well as an integral over three-momenta. This sum may be evaluated using the following technique. Let us first define a Fourier-transformed propagator with respect to $\omega_n = 2n\pi T$, for bosons, as

$$\Delta_B(\tau, \mathbf{k}) = T \sum_{n=-\infty}^{\infty} e^{-i\omega_n\tau} \mathcal{D}_0(\omega_n, \mathbf{k}) \quad (9.5)$$

The sum over discrete frequencies is easily done by using the contour integration technique of Chapter 3. The result is

$$\Delta_B(\tau, \mathbf{k}) = \frac{1}{2|\mathbf{k}|} \left\{ [1 + N_B(\mathbf{k})] e^{-|\mathbf{k}|\tau} + N_B(\mathbf{k}) e^{|\mathbf{k}|\tau} \right\} \quad (9.6)$$

where $N_B(\mathbf{k}) = 1/[\exp(|\mathbf{k}|/T) - 1]$. The inverse of (9.5) is

$$\mathcal{D}_0(\omega_n, \mathbf{k}) = \int_0^\beta d\tau e^{i\omega_n\tau} \Delta_B(\tau, \mathbf{k}) \quad (9.7)$$

It is easy to verify that the boson propagator in imaginary time has the following properties:

$$\Delta_B(\tau - \beta, \mathbf{k}) = \Delta_B(-\tau, \mathbf{k}) = \Delta_B(\tau, \mathbf{k}) \quad (9.8)$$

A similar analysis for fermions, with $\omega_n = (2n + 1)\pi T$, yields the intuitive result

$$\Delta_F(\tau, \mathbf{k}) = T \sum_{n=-\infty}^{\infty} \frac{e^{-i\omega_n\tau}}{\omega_n^2 + \mathbf{k}^2} = \frac{1}{2|\mathbf{k}|} \left\{ [1 - N_F(\mathbf{k})] e^{-|\mathbf{k}|\tau} - N_F(\mathbf{k}) e^{|\mathbf{k}|\tau} \right\} \quad (9.9)$$

where $N_F(\mathbf{k}) = 1/[\exp(|\mathbf{k}|/T) + 1]$.

The usefulness of this approach is easily illustrated for the case of one-loop integrals. There, each internal propagator (we concentrate on bosons for simplicity) is written as an integral over τ as in (9.7). Evaluating the sum over discrete frequencies will create a delta function in τ . The overall integral over imaginary time can be done directly. Then the contribution of order T^2 is easy to pick out. A few examples will help to illustrate the procedure.

In a tadpole self-energy one has to evaluate

$$\begin{aligned} T \sum_{n=-\infty}^{\infty} \int \frac{d^3k}{(2\pi)^3} \mathcal{D}_0(\omega_n, \mathbf{k}) &= T \sum_{n=-\infty}^{\infty} \int \frac{d^3k}{(2\pi)^3} \int_0^\beta d\tau e^{i\omega_n \tau} \Delta_B(\tau, \mathbf{k}) \\ &= \int \frac{d^3k}{(2\pi)^3} \Delta_B(\tau = 0, \mathbf{k}) \\ &= \int \frac{d^3k}{(2\pi)^3} \frac{1}{2|\mathbf{k}|} [1 + 2N_B(\mathbf{k})] \end{aligned} \tag{9.10}$$

The first term corresponds to the usual $T = 0$ ultraviolet divergence and is removed by renormalization. Rewriting the result for the remaining term we get

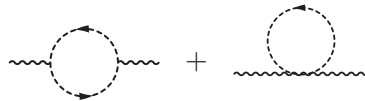
$$T \sum_{n=-\infty}^{\infty} \int \frac{d^3k}{(2\pi)^3} \mathcal{D}_0(\omega_n, \mathbf{k}) \approx \frac{1}{12} T^2 \tag{9.11}$$

The approximation sign means that equality holds “in the hard thermal loop (HTL) limit”. Here this is actually an exact result.

Another example is that of the photon self-energy in scalar QED. Let us write the Lagrangian that governs the behavior of the scalar field ϕ and of the photon field A_μ as

$$\mathcal{L} = (D_\mu \phi)^* D^\mu \phi - \frac{1}{4} F_{\mu\nu} F^{\mu\nu} - \frac{1}{2\rho} (\partial^\mu A_\mu)^2 \tag{9.12}$$

where ρ is the gauge-fixing parameter, discussed in Chapter 5. Recall that $D_\mu = \partial_\mu + ieA_\mu$. The Feynman diagrams that contribute to the first-order self-energy are



In Euclidean space the photon self-energy is

$$\begin{aligned} \Pi^{\mu\nu}(\omega_m, \mathbf{p}) &= -e^2 T \sum_n \int \frac{d^3k}{(2\pi)^3} \frac{(2k+p)^\mu (2k+p)^\nu}{(\omega_n^2 + \mathbf{k}^2) [(\omega_m + \omega_n)^2 + |\mathbf{p} + \mathbf{k}|^2]} \\ &+ 2 \delta^{\mu\nu} e^2 T \sum_n \int \frac{d^3k}{(2\pi)^3} \frac{1}{\omega_n^2 + \mathbf{k}^2} \end{aligned} \tag{9.13}$$

To facilitate the usage of noncovariant propagators, this may be written as

$$\begin{aligned} \Pi^{\mu\nu}(\omega_m, \mathbf{p}) = & -e^2 T \sum_n \int \frac{d^3 k}{(2\pi)^3} \frac{(k - q)^\mu (k - q)^\nu}{(\omega_n^2 + \mathbf{k}^2)(\omega_q^2 + \mathbf{q}^2)} \\ & + 2\delta^{\mu\nu} e^2 T \sum_n \int \frac{d^3 k}{(2\pi)^3} \frac{1}{\omega_n^2 + \mathbf{k}^2} \end{aligned} \tag{9.14}$$

where $\mathbf{q} = \mathbf{p} - \mathbf{k}$ and $\omega_q = \omega_m - \omega_n$.

Concentrating on the finite-temperature contributions, and recalling that the temperature-independent divergent parts are regulated using the same techniques that operate at zero temperature, we may write

$$\Pi^{\mu\nu} = F P_L^{\mu\nu} + G P_T^{\mu\nu} \tag{9.15}$$

which is now in Minkowski space. The analysis and the results are very similar to those of electronic QED that were derived in Chapters 5 and 6. The quantities P_L and P_T are the familiar longitudinal and transverse projection tensors. The scalar functions F and G are inferred as follows:

$$F = \Pi^{\mu\nu} P_{L\mu\nu} , \tag{9.16}$$

$$G = \frac{1}{2} \Pi^{\mu\nu} P_{T\mu\nu} \tag{9.17}$$

Note that the transversality of $\Pi^{\mu\nu}$ ($k_\mu \Pi_L^{\mu\nu} = k_\mu \Pi_T^{\mu\nu} = 0$) is manifest, as required by current conservation. Writing $F = (p^2/\mathbf{p}^2) \Pi^{00}$ and using (9.15) and the fact that the integral defining the scalar function will be dominated by the hard momentum scale $k \sim T$, we get

$$F \approx \frac{e^2 T^2}{3} \left(1 - \frac{p_0^2}{\mathbf{p}^2} \right) \left[1 - \frac{p_0}{2|\mathbf{p}|} \ln \left(\frac{p_0 + |\mathbf{p}|}{p_0 - |\mathbf{p}|} \right) \right] \tag{9.18}$$

where for this discussion $p_0 = i\omega_m$, and $p^2 = p_0^2 - \mathbf{p}^2 = -(\omega_m^2 + \mathbf{p}^2)$. Here again the approximation sign is to be interpreted as meaning “in the HTL limit”. Similarly, one may show that

$$G \approx \frac{1}{2} \left(\frac{e^2 T^2}{3} - F \right) \tag{9.19}$$

From this analysis of the HTL contribution in scalar QED, some new aspects are immediately apparent. Unlike $\lambda\phi^4$ theory, the self-energy is not only temperature dependent but now also momentum dependent. Also, the self-energy can develop an imaginary part when the kinematics are such that $|\mathbf{p}| > p_0 > -|\mathbf{p}|$. This situation corresponds to that of Landau damping, where one particle is emitted from the thermal medium and another is absorbed.

The reader will undoubtedly have noticed that writing propagators in frequency-momentum space and then performing a Fourier transform to

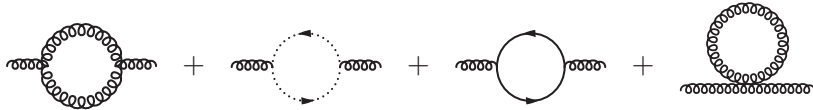
imaginary time is but another method of doing the frequency sums. In some cases, it has advantages over the direct contour integral technique. However, the trick turns out to be useful only for loop diagrams; for tree-level diagrams little is gained by going over to the imaginary time–momentum domain.

The examples considered here can be used to extract some rules for the evaluation of the HTLs. Following Braaten and Pisarski, one might generalize the procedure to the evaluation of N -point functions in one-loop amplitudes for QCD at finite temperature. Before one proceeds to the more general case, it is instructive to evaluate explicitly the HTL contribution to the gluon self-energy. This calculation was first performed by Kalashnikov and Klimov [3] and Weldon [4].

We shall perform the QCD calculation in the Coulomb gauge ($\nabla \cdot \mathbf{A}^a = 0$), with a as color index. Even though this gauge is a little awkward for many applications, owing partly to the fact that it is noncovariant, it has certain advantages at finite temperature. We will see some of those shortly. Of course, the result of a calculation of any physical quantity should be gauge invariant. Recall that the bare gluon propagator in the Coulomb gauge is (omitting the color indices)

$$\mathcal{D}^{\mu\nu} = -\frac{1}{p^2} P_T^{\mu\nu} - \frac{1}{\mathbf{p}^2} u^\mu u^\nu \tag{9.20}$$

A gauge-fixing term $(\nabla \cdot \mathbf{A}^a)^2/2\rho$ could be added but would not change the analysis that follows. At one-loop order, the gluon self-energy is obtained by computing the Feynman diagrams in the following figure:



Note that the ghost propagator in the Coulomb gauge is $1/\mathbf{p}^2$, omitting color indices. Thus, ghost fields are static in the Coulomb gauge: they do not propagate. The same is true of the longitudinal gluons, another convenient feature. Hence there are advantages in using the Coulomb gauge in an application like the one considered here. In gauges with propagating unphysical degrees of freedom, the contributions from ghosts and longitudinal gluons cancel each other only in the final stages of a calculation. Therefore, the choice of the Coulomb gauge makes the computation of the second diagram in the figure above unnecessary.

The first diagram in the figure generates a contribution to the self-energy that is

$$\Pi = -\frac{g^2 N}{2} T \sum_n \int \frac{d^3 k}{(2\pi)^3} \Gamma \mathcal{D} \Gamma \mathcal{D} \tag{9.21}$$

The prefactor is easily understood. The factor 1/2 comes from a combination of the coefficient in the perturbative expansion of the thermodynamic potential, the numerical factors associated with the triple-gluon vertex, and combinatorics. The factor N comes from a color trace. In the HTL limit, the loop momentum constitutes a hard scale. In that limit, the vertex functions can be rewritten as

$$\begin{array}{c}
 p(\alpha, a) \\
 \downarrow \\
 \begin{array}{c}
 \text{---} \\
 \uparrow \quad \downarrow \quad \uparrow \\
 (k-p)(\beta, b) \quad \quad \quad k(\gamma, c)
 \end{array}
 \end{array}
 \approx igf_{abc} (g_{\beta\gamma} 2k_\alpha - g_{\alpha\beta} k_\gamma - g_{\gamma\alpha} k_\beta)$$

where k is the hard loop momentum. Inserting this vertex and using the high-temperature limit, one obtains the HTL limit of the contribution of the first self-energy diagram in frequency–momentum space:

$$\begin{aligned}
 \Pi^{\mu\nu}(\omega_m, \mathbf{p}) \approx & 4g^2 NT \sum_n \int \frac{d^3k}{(2\pi)^3} k^\mu k^\nu \mathcal{D}_0(k) \mathcal{D}_0(p-k) \\
 & + g^2 NT \sum_n \int \frac{d^3k}{(2\pi)^3} \delta^{\mu i} \delta^{\nu j} \mathcal{D}_{ij}(k)
 \end{aligned}
 \tag{9.22}$$

In a similar fashion one may compute the self-energy corresponding to the four-gluon vertex and to the quark–antiquark loop. The sum of these different contributions is written in Euclidean space as

$$\begin{aligned}
 \Pi^{\mu\nu}(\omega_m, \mathbf{p}) \approx & 4g^2 \left(N + \frac{1}{2} N_f \right) \left(T \sum_n \int \frac{d^3k}{(2\pi)^3} k^\mu k^\nu \mathcal{D}_0(k) \mathcal{D}_0(p-k) \right. \\
 & \left. - \frac{1}{2} \delta^{\mu\nu} T \sum_n \int \frac{d^3k}{(2\pi)^3} \mathcal{D}_0(k) \right)
 \end{aligned}
 \tag{9.23}$$

The high-temperature limit of the gluon self-energy takes exactly the same form as (9.18), (9.19) with the replacement of the overall factor $e^2 T^2/3$ by the square of the color electric mass m_{el}^2 . The latter is

$$m_{\text{el}}^2 = \frac{1}{3} g^2 \left[NT^2 + \frac{1}{2} \sum_f \left(T^2 + \frac{3}{\pi^2} \mu_f^2 \right) \right]
 \tag{9.24}$$

where the sum refers to the quark flavors f , which may have differing chemical potentials. The energy and momentum dependence of the gluon self-energy, in this limit, is also identical to that of electronic QED, as analyzed in Section 6.7. It follows that the functional form of the dispersion relation is the same as for photons, at least to lowest order in the coupling constants.

Upon generalizing our result from self-energies to an arbitrary N -point function, considerable progress is made by observing that the momentum-independent term in (9.22) is specific to the self-energy topology. For example, it will be absent in the HTL limit of the three-point functions.

Next consider the N -gluon amplitude in the Coulomb gauge. One of the Feynman diagrams is shown in the following figure. (The complete HTL calculation also needs a diagram with an internal quark loop.)



In the usual notation this N -point amplitude is proportional to

$$T \sum_n \int \frac{d^3k}{(2\pi)^3} k^{\mu_1} \dots k^{\mu_N} \mathcal{D}_0(k) \mathcal{D}_0(p_1 - k) \dots \mathcal{D}_0(p_{N-1} - k) \quad (9.25)$$

Insert the noncovariant propagators and do the frequency sum. One of the resulting terms is

$$\int d^3k \frac{k^{\mu_1} \dots k^{\mu_N}}{|\mathbf{k}| |\mathbf{p}_1 - \mathbf{k}| \dots |\mathbf{p}_{N-1} - \mathbf{k}|} [N_B(\mathbf{k}) - N_B(\mathbf{p}_1 - \mathbf{k})] \times [(p_1^0 - |\mathbf{k}| + |\mathbf{p}_1 - \mathbf{k}|) \dots (p_{N-1}^0 - |\mathbf{k} - \mathbf{p}_{N-1}| + |\mathbf{k}|)]^{-1} \quad (9.26)$$

The structure of the integrand can be understood as follows. The N momenta in the first denominator come from the denominators of the Fourier transform of the Euclidean propagators, (9.6); the N gluon momenta in the numerator come from the triple-gluon coupling, which is linear in momentum. The energy denominators come from integrating over the different imaginary time variables associated with the use of (9.7). There are only $N - 1$ of them, as the first integral was used in conjunction with the delta function generated by the frequency sum. As argued previously, hard thermal loops occur when the integrating region is hard, of order T . We may get an estimate of the magnitude of (9.26) when the external momentum is soft, of order gT . In that limit

$$k \sim T \quad |\mathbf{p}_i - \mathbf{k}| \sim T \quad |\mathbf{k}| - |\mathbf{p} - \mathbf{k}| \sim |\mathbf{p}|$$

Now we use $N_B(\mathbf{k}) - N_B(\mathbf{p} - \mathbf{k}) \approx |\mathbf{p}| z dN_B(\mathbf{k})/dk$, with $z = \hat{\mathbf{p}} \cdot \hat{\mathbf{k}}$. Putting all this together, and recalling that there is one power of the coupling constant at each vertex, the amplitude for N external gluons is $g^N T^2 / |\mathbf{p}|^{N-2}$. The tree-level diagram for the N -point gluon amplitude is easier to estimate: it contains $N - 2$ vertices and $N - 3$ propagators. Its magnitude is thus $g^{N-2} / |\mathbf{p}|^{N-4}$. Clearly, when $|\mathbf{p}| \sim gT$ in the one-loop N -gluon amplitude, its magnitude is that of the tree-level contribution

and therefore has to be included in a consistent calculation. Therefore a resummation is required.

A set of rules for the power-counting of one-loop diagrams, first established by Braaten and Pisarski, may be inferred from the above analysis. They are summarized here for the case where all external momenta are soft.

- 1 The measure of the integral over the loop momentum is of magnitude T^3 .
- 2 One propagator does not contribute an energy denominator since it is used in the integral over the delta function in imaginary time. Thus, there is a factor $1/T$ for the first propagator from the denominator of (9.6), and a factor $1/gT$ for each additional propagator owing to Landau damping contributions.
- 3 Each k^μ in the numerator, from vertices or fermion propagators, is replaced by T .
- 4 For loops with at least two propagators, if the latter represent fields of the same statistics, an extra factor of p/T appears owing to the cancellation of distribution functions.

Note that the $N = 2$ case does require separate consideration. This can be seen upon examination of the tadpole diagram in the scalar QED example, and also in the computation of the gluon self-energy in the Coulomb gauge. It is now also clear why loops with ghost fields will not contribute to the HTL term in the Coulomb gauge: because they are nonpropagating they cannot generate the term $1/gT$ associated with Landau damping. More specifically, the transverse gluon propagator will have a contribution $1/T \times 1/gT$, whereas a field with propagator $\sim 1/\mathbf{k}^2$ will have a contribution $1/T^2$, suppressed by one power of g . It is also useful to note here that these rules assume that the N -point functions are linear in the thermal distribution functions, whereas from (9.6) it would appear that powers of the distribution function would arise. This power would be the same as the number of propagators. However, in the final result a cancellation always yields a single power of N_B or N_F . This fact is most easily seen when the frequency sum is performed by the technique of contour integration. Indeed, considering (3.40) one sees that each pole residue gets multiplied by a single distribution function. Finally, we note that there is no HTL amplitude with external ghost fields.

9.2 Hard thermal loops and Ward identities

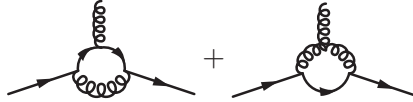
In the case of a gauge theory we know that N -point functions are related to $(N - 1)$ -point functions by Ward identities. At high temperature,

where HTLs give the leading contribution, we shall verify that Ward identities are indeed satisfied. This is a useful check on the method.

As an exercise, we can first check whether the HTL limit of the photon self-energy in scalar QED satisfies a Ward identity; verification is immediate, $p^\mu \Pi_{\mu\nu}(\omega_m, \mathbf{p}) = 0$. The same observation can be made for the gluon self-energy we obtained previously. It suffices to calculate explicitly three-point and four-point functions in order to generalize to a given topology at some order of the coupling. For example, the three-gluon amplitude will receive contributions from a pure gluon loop and from a quark loop. With the rules, the HTL limit of their sum can be obtained, and it is

$$\Gamma^{\mu\nu\sigma} \approx -8g^2 \left(N + \frac{1}{2}N_f \right) T \times \sum_n \int \frac{d^3k}{(2\pi)^3} k^\mu k^\nu k^\sigma \mathcal{D}_0(k) \mathcal{D}_0(p_1 - k) \mathcal{D}_0(p_2 + k) \quad (9.27)$$

Note that the momentum-labeling convention in the vertex is such that $p_1 + p_2 + p_3 = 0$. Similarly, the HTL limit of the two-quark one-gluon vertex is obtained through the evaluation of



and is

$$\Gamma_{2q-1g}^\mu \approx -4g^2 C_f \gamma_\nu T \sum_n \int \frac{d^3k}{(2\pi)^3} k^\mu k^\nu \mathcal{D}_0(k) \mathcal{D}_0(p_1 - k) \mathcal{D}_0(p_2 + k) \quad (9.28)$$

where $C_f = (N^2 - 1)/2N$ and N is the number of colors.

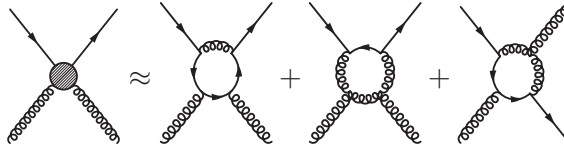
The Ward identities can be derived in a straightforward fashion from the properties of the three-point and four-point functions in the HTL limit. Besides the transversality condition already mentioned, they are

$$\begin{aligned} p_{3\gamma} \Gamma^{\alpha\beta\gamma}(p_1, p_2, p_3) &= \Pi^{\alpha\beta}(p_1) - \Pi^{\alpha\beta}(p_2) \\ p_{3\mu} \Gamma_{2q-1g}^\mu(p_1, p_2, p_3) &= \Sigma(p_1) - \Sigma(p_2) \end{aligned} \quad (9.29)$$

where $\Sigma(p)$ is the high-temperature quark self-energy. Similarly, the four- and three-point functions, in the HTL limit, are related by

$$\begin{aligned} p_{4\delta} \Gamma^{\alpha\beta\gamma\delta}(p_1, p_2, p_3, p_4) &= \Gamma^{\alpha\beta\gamma}(p_1 + p_4, p_2, p_3) \\ &\quad - \Gamma^{\alpha\beta\gamma}(p_1, p_2 + p_4, p_3) \\ p_{4\beta} \Gamma_{2q-2g}^{\alpha\beta}(p_1, p_2, p_3, p_4) &= \Gamma_{2q-1g}^\alpha(p_1 + p_4, p_2, p_3) \\ &\quad - \Gamma_{2q-1g}^\alpha(p_1, p_2 + p_4, p_3) \end{aligned} \quad (9.30)$$

where a trace over the color indices of the two gluons has been taken. It is now apparent that effective vertices can and will exist in cases where no bare vertex is defined. For example, the 1PI vertex between a pair of quarks and a pair of gluons, $\Gamma_{2q-2g}^{\mu\nu}$, will consist solely of one-loop HTL contributions, as is obvious from the figure:



A consequence of the fact that hard thermal loops obey Ward identities similar to those of tree amplitudes is that their generating functional is a gauge-invariant functional of the quark and gauge fields.

9.3 Hard thermal loops and effective perturbation theory

We have seen that, owing to hard thermal loops, some Feynman diagrams that are superficially higher order in the coupling constant will have the same magnitude as tree-level diagrams in finite-temperature field theories. We have also seen how to evaluate the HTL contributions. We can employ this knowledge to resum HTLs into an effective theory. In this formalism bare vertices and propagators will be replaced by effective vertices and propagators, which are obtained via a HTL resummation.

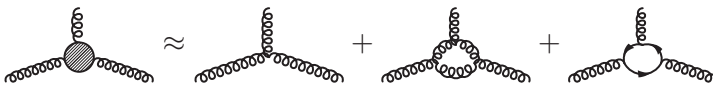
Using the Schwinger–Dyson equation one may define an effective gluon inverse propagator in terms of the bare one as

$$(\mathcal{D}^*)_{\mu\nu}^{-1} = p^2 g_{\mu\nu} - p_\mu p_\nu + \Pi_{\mu\nu}^* \tag{9.31}$$

where the self-energy is evaluated in the HTL limit. An equivalent expression exists for quarks, the inverse propagator being related to the self-energy. The effective three-gluon vertex can be constructed similarly:

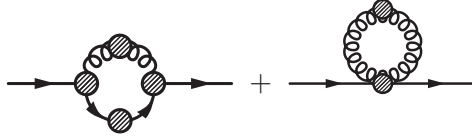
$$\Gamma^{*\mu\nu\sigma}(p_1, p_2, p_3) = \Gamma_0^{\mu\nu\sigma}(p_1, p_2, p_3) + \delta\Gamma^{\mu\nu\sigma}(p_1, p_2, p_3) \tag{9.32}$$

where the finite-temperature contribution (the second term on the right-hand side) is evaluated in the HTL limit. The contributions to the three-point function, in a ghost-free gauge, are represented by



This procedure is generalized to more complicated topologies. As noted in the previous section, HTL effective vertices can exist in the absence of their bare counterparts. If all the external momenta are of order gT then the HTL self-energies are of the same order as the bare inverse propagators; the same statement holds true for vertices. Therefore, in

the evaluation of a loop contribution, propagators and vertices need to be of the effective kind for the kinematical region where the loop momentum is soft. An example is that of the one-loop quark self-energy



where the blobs denote effective quantities.

One might formalize the effective perturbation theory one step further by starting with effective Lagrangians. One can show [5] that the effective Lagrangian for gluonic hard thermal loops is

$$\mathcal{L} = -\frac{1}{2}m_{\text{el}}^2 \text{Tr} \left[F_{\mu\nu}(x) \int \frac{d\Omega}{4\pi} \frac{\hat{k}^\nu \hat{k}^\lambda}{(\hat{k} \cdot D)^2} F_\lambda^\mu(x) \right] \tag{9.33}$$

Here the trace runs over color indices, $F_{\mu\nu} = F_{\mu\nu}^a G_a$ where the G_a are the generators of the group, and $\hat{k} = (-i, \hat{\mathbf{k}})$ (in Minkowski space). The integration over solid angle refers to the direction $\hat{\mathbf{k}}$. Also, $D^\mu = \partial^\mu + igA^\mu$ is the covariant derivative ($A^\mu = A_a^\mu G_a$). Similarly the effective Lagrangian for fermionic hard thermal loops is

$$\mathcal{L} = m_q^2 \bar{\psi}(x) \gamma_\mu \int \frac{d\Omega}{4\pi} \frac{\hat{k}^\mu}{\hat{k} \cdot D} \psi(x) \tag{9.34}$$

with

$$m_q^2 = \frac{N^2 - 1}{16N} g^2 \left(T^2 + \frac{\mu^2}{\pi^2} \right) \tag{9.35}$$

9.4 Spectral densities

It is interesting to know where the spectral weights are concentrated for various operators within the hard thermal loop approximation. Here we shall focus on the quark spectral densities since they will be used in Chapter 14 to compute the rate of photon emission from the quark–gluon plasma formed in high-energy heavy ion collisions.

The quark self-energy in the HTL limit may be immediately inferred from the electron self-energy given in Section 6.8. The only difference is the change in the numerical factor in the fermion–vector meson vertex. The quark propagator is

$$\mathcal{G}^*(p) = \mathcal{G}_+^*(p) \frac{\gamma_0 - \hat{\mathbf{p}} \cdot \boldsymbol{\gamma}}{2} + \mathcal{G}_-^*(p) \frac{\gamma_0 + \hat{\mathbf{p}} \cdot \boldsymbol{\gamma}}{2} \tag{9.36}$$

where

$$\mathcal{G}_{\pm}^*(p) = \left\{ -p_0 \pm |\mathbf{p}| + \frac{m_q^2}{|\mathbf{p}|} \left[Q_0 \left(\frac{p_0}{|\mathbf{p}|} \right) \mp Q_1 \left(\frac{p_0}{|\mathbf{p}|} \right) \right] \right\}^{-1} \quad (9.37)$$

The functions Q_0 and Q_1 are the Legendre functions of the second kind, namely

$$Q_0(z) = \frac{1}{2} \ln \left(\frac{1+z}{1-z} \right) \quad Q_1(z) = zQ_0(z) - 1 \quad (9.38)$$

The effective quark mass was given in (9.35). In the limit $g \rightarrow 0$ we recover the bare quark propagator.

It is a straightforward exercise to compute the spectral densities for the functions \mathcal{G}_{\pm}^* . They are

$$\rho_{\pm}^*(\omega, \mathbf{p}) = \frac{\omega^2 - \mathbf{p}^2}{2m_q^2} [\delta(\omega - \omega_{\pm}(\mathbf{p})) + \delta(\omega + \omega_{\mp}(\mathbf{p}))] + \beta_{\pm}(\omega, \mathbf{p})\theta(\mathbf{p}^2 - \omega^2) \quad (9.39)$$

with

$$\beta_{\pm}(\omega, \mathbf{p}) = \frac{1}{2} m_q^2 (|\mathbf{p}| \mp \omega) \left(\left\{ |\mathbf{p}|(\omega \mp |\mathbf{p}|) - m_q^2 \left[Q_0 \left(\frac{\omega}{|\mathbf{p}|} \right) \mp Q_1 \left(\frac{\omega}{|\mathbf{p}|} \right) \right] \right\}^2 + \left[\frac{1}{2} \pi m_q^2 \left(1 \mp \frac{\omega}{|\mathbf{p}|} \right) \right]^2 \right)^{-1} \quad (9.40)$$

The $\omega_{\pm}(\mathbf{p})$ represent the two branches of the dispersion relation for quarks, essentially as discussed in Section 6.8. They are, of course, determined by the poles of $\mathcal{G}_{\pm}^*(\omega, \mathbf{p})$. The functions β_{\pm} represent branch cuts that give rise to Landau damping, which is possible when $|\omega| < |\mathbf{p}|$.

9.5 Kinetic theory

The connection between kinetic theory and the HTL formalism is at first sight surprising and mysterious. However, once we realize that small deviations from local thermal equilibrium may be described by either kinetic theory or by linear response theory, the connection may be viewed as different manifestations of the same physics.

The connection can be initiated by considering the elementary example of an ensemble of charged classical particles. Assuming that hard collisions can be neglected, and that the particles thus interact only through average electric and magnetic fields, one can write an equation for the time evolution of the single-particle phase-space distribution $f(\mathbf{x}, \mathbf{p}, t)$:

$$\frac{\partial f}{\partial t} + \mathbf{v} \cdot \frac{\partial f}{\partial \mathbf{x}} + \mathbf{F} \cdot \frac{\partial f}{\partial \mathbf{p}} = 0 \quad (9.41)$$

Here \mathbf{v} is a velocity and \mathbf{F} is the Lorentz force. Note that in general the single-particle distribution function depends on time, on the position and on the momentum. This transport-type equation can be derived by requiring the total time derivative to vanish in the absence of hard collisions: a statement of Liouville's theorem. This equation is the collisionless Boltzmann or Vlasov equation. The derivation is completed by using the appropriate Lagrangian for electromagnetic interactions as well as Hamilton's equations. For an electromagnetic plasma in equilibrium the distribution functions will not depend on the spacetime coordinates and will be isotropic in momentum space. Keeping those facts in mind, let us slightly perturb the distribution function $f^{(0)}$:

$$f(\mathbf{x}, \mathbf{p}, t) = f^{(0)}(|\mathbf{p}|) + \delta f(\mathbf{x}, \mathbf{p}, t) \quad (9.42)$$

Then, to first order in the modification of the distribution function,

$$\left(\frac{\partial}{\partial t} + \mathbf{v} \cdot \frac{\partial}{\partial \mathbf{x}} \right) \delta f(\mathbf{x}, \mathbf{p}, t) = -e\mathbf{E} \cdot \mathbf{v} \frac{df^{(0)}(|\mathbf{p}|)}{d\epsilon} \quad (9.43)$$

where ϵ is the energy of the particle of charge e . Assuming that the perturbation is switched on adiabatically, one may solve for the out-of-equilibrium part of the distribution function:

$$\delta f(\mathbf{x}, \mathbf{p}, t) = -e \frac{df^{(0)}(|\mathbf{p}|)}{d\epsilon} \int_{-\infty}^t dt' e^{-\eta(t-t')} \mathbf{v} \cdot \mathbf{E}(\mathbf{x} - \mathbf{v}(t-t'), t') \quad (9.44)$$

This leads to an induced current

$$j_{\text{ind}}^{\mu}(\mathbf{x}, t) = e \int \frac{d^3p}{(2\pi)^3} v^{\mu} \delta f(\mathbf{x}, \mathbf{p}, t) \quad (9.45)$$

where $v^{\mu} = (1, \mathbf{v})$. Finally, relating the polarization tensor to the induced current via

$$j_{\text{ind}}^{\mu}(x) = \int d^4y \Pi^{\mu\nu}(x-y) A_{\nu}(y) \quad (9.46)$$

one obtains the following results in frequency–momentum space:

$$\begin{aligned} \Pi_{00}(\omega_m, \mathbf{p}) &= -\frac{e^2 T^2}{3} \left(1 - \int \frac{d\Omega}{4\pi} \frac{i\omega_m}{i\omega_m - \mathbf{q} \cdot \hat{\mathbf{v}}} \right) \\ \Pi_{ij}(\omega_m, \mathbf{p}) &= \frac{e^2 T^2}{3} \int \frac{d\Omega}{4\pi} \frac{i\omega_m \hat{v}_i \hat{v}_j}{i\omega_m - \mathbf{q} \cdot \hat{\mathbf{v}}} \end{aligned} \quad (9.47)$$

We have made the assumption that the particles are massless, in which case their velocity vector is a unit vector $\hat{\mathbf{v}}$. The integrals in (9.47) are then over the orientation of the unit velocity vector. Remarkably, the result above is in fact the HTL contribution to the one-loop photon polarization tensor in QED. A direct calculation to show this is straightforward.

An important feature emerges here that generalizes to both the quantum domain and to nonabelian quantum field theories. This feature is that the Vlasov equation is an effective equation of motion for the soft modes of the plasma and corresponds to the fact that the hard thermal loops are obtained by isolating the leading-order contributions to one-loop diagrams with soft external lines. Put another way, the induced current calculated from the solutions of the Vlasov equation generates directly the HTL contribution.

Since in QED the HTL in the vacuum polarization tensor could be obtained by using classical transport theory, one could attempt a similar treatment for QCD. This approach appears promising, as HTLs represent the interaction of energetic quanta with weak mean fields. The hard thermal effects should then be driven by thermal fluctuations that can be cast in a classical framework. The starting point consists of considering a set of particles carrying nonabelian $SU(N)$ color charge Q^a . One may write down the time evolution equations for the space-momentum coordinates of those particles. An important difference arises immediately in QCD: the particles may exchange color with the fields with which they interact. There needs to be an equation of motion for the color quantum number. The set (x, p, Q^a) can be thought of as an augmented phase space. Note that, except for Q^a , the elements of this set are now four-vectors.

The dynamical evolution of these phase-space variables is dictated by S. K. Wong's equations [6]. They can be derived by starting with the Dirac equation, suitably generalized to include QCD, finding the equations of motion for the operators, and then letting $\hbar \rightarrow 0$. One obtains

$$\begin{aligned} m \frac{dx^\mu}{d\tau} &= p^\mu & m \frac{dp^\mu}{d\tau} &= gQ^a F_a^{\mu\nu} p_\nu \\ m \frac{dQ^a}{d\tau} &= -g f^{abc} p^\mu A_\mu^b Q^c \end{aligned} \quad (9.48)$$

As usual $F_{\mu\nu}^a$ is the field strength tensor, g is the strong coupling constant, and the f^{abc} are the structure constants of the group. These equations can be generalized to include spin, but this is not important for the present discussion. In the collisionless case, the proper-time total derivative of the phase-space density should vanish: $df(x, p, Q)/d\tau = 0$. Using the equations of motion presented above, one obtains the Boltzmann equation in the absence of collisions,

$$p^\mu \left(\frac{\partial}{\partial x^\mu} - gQ_a F_{\mu\nu}^a \frac{\partial}{\partial p_\nu} - g f_{abc} A_\mu^b Q^c \frac{\partial}{\partial Q_a} \right) f(x, p, Q) = 0 \quad (9.49)$$

Together with the Yang–Mills equation, $(D_\nu F^{\mu\nu})^a = J^{\mu a}$ (where the covariant derivative is $D_\mu^{ac} = \partial_\mu \delta^{ac} + g f^{abc} A_\mu^b$), one obtains a

self-consistent set of nonabelian Vlasov equations. The net current is $J^{\mu a} = \sum j^{\mu a}$, where the sum runs over all species and spins. The space-time coordinates are implicit. More explicitly,

$$j^{\mu a}(x, p) = g \int dQ p^\mu Q^a f(x, p, Q) \quad (9.50)$$

Physical states are guaranteed if the appropriate constraints are incorporated in the measure of the augmented phase space. In the limit of vanishing masses,

$$dQ = d^8 Q \delta(Q^a Q_a - q_2) \delta(d_{abc} Q^a Q^b Q^c - q_3) \quad (9.51)$$

$$dP = \frac{d^4 p}{(2\pi)^3} 2\theta(p_0) \delta(p^2) \quad (9.52)$$

The first equation is specific to SU(3) and ensures the invariance of the Casimir constants. The d_{abc} are the totally symmetric group constants. The second equation makes positivity manifest along with the on-shell requirement.

Specializing in small departures from equilibrium, one may write

$$f = f^{(0)} + g f^{(1)} + g^2 f^{(2)} + \dots \quad (9.53)$$

To first order in the coupling, the transport equation reduces to

$$p^\mu \left(\frac{\partial}{\partial x^\mu} - g f^{abc} A_\mu^b Q_c \frac{\partial}{\partial Q^a} \right) f^{(1)} = p^\mu Q_a F_{\mu\nu}^a \frac{\partial}{\partial p_\nu} f^{(0)} \quad (9.54)$$

Arguments that are phase-space variables are once again left implicit.

Integrating by parts, using the definition of the current at a given order in terms of the distribution function, (9.50), and summing over the N_f quarks, N_f antiquarks, and the $N^2 - 1$ gluons and their physical spin states, one gets

$$[p \cdot D J^\mu(x, p)]^a = 2g^2 p^\mu p^\nu F_{\nu 0}^a \frac{d}{dp_0} [N N_B(p_0) + N_f N_F(p_0)] \quad (9.55)$$

Kelly *et al.* [7], as well as Taylor and S. M. H. Wong [8] have shown that a solution of the above can be obtained in a functional form: $J^\mu(x) = -\delta\Gamma(A)/\delta A_\mu = -G^a \delta\Gamma(A)/\delta A_\mu^a$. The generating functional is

$$\Gamma = \frac{m_{\text{el}}^2}{2} \int d^4 x A_0^a(x) A_0^a(x) - \int \frac{d\Omega}{(2\pi)^3} W(A) \quad (9.56)$$

where an explicit expression for W is given in [8]. This generating functional is consistent with the effective Lagrangians we wrote down earlier.

A field-theoretic procedure can also be invoked to derive the results above. Following Blaizot and Iancu [9], the field equations of motion may be obtained by functional differentiation of the nonabelian generating functional. However, by definition this procedure does not produce

gauge-invariant equations of motion. Indeed, the original Lagrangian in the action has to be gauge-fixed. This is not a problem, as physical results will not depend on the choice of gauge. However, intermediate steps that are gauge independent do permit a clearer physical interpretation. A method that circumvents this annoyance is that of the background gauge field [10], where the gauge field is split into a classical background field, identifiable as a mean field, and a fluctuating quantum field. Then a mean field approximation, where hard degrees of freedom interact with softer mean fields, together with an extraction of terms of leading order in g , is performed. Care has to be taken to preserve the gauge symmetry in those procedures. As in the classical limit, one allows first-order fluctuations in the density matrices, the Wigner transforms of which have many of the properties of classical phase-space distributions. The transport equations thus obtained yield (9.55). Note that practical applications typically involve the evaluation of quantities like the polarization tensor. This may be obtained from the current in the case of weak fields or, equivalently, in the linear response limit by a functional derivative of (9.46). Finally, the formal manipulations in [9] have greatly clarified the physical nature of hard thermal loops. As already mentioned, the high-temperature limit does permit an ordering of scales. One starts with an identification of plasma particles that have typical momenta of order T . Soft collective degrees of freedom then appear, which carry the same quantum numbers as the primordial constituents but which have typical momenta of the order of gT . This scale separation allows for the derivation of a kinetic equation for the plasma particles, the solution of which provides a generating functional for the hard thermal loops. Therefore, hard thermal loops describe long-wavelength collective excitations of the thermal particles. A natural consequence of this fact is that HTL perturbation theory is useful for the evaluation of physical quantities that are only sensitive to scales of the order of gT . Many other observables will be sensitive to scattering processes whose treatment will go beyond hard thermal loops.

9.6 Transport coefficients

In Section 6.9 we discussed the general Kubo formulae for transport coefficients. For completeness we quote here the values for the shear viscosity and flavor diffusion constant for QCD at high temperature. They were computed to lowest order in the gauge coupling but to all orders in the logarithm of the coupling by Arnold, Moore and Yaffe [11]. For the pure gauge theory without dynamical quarks the results are

$$D = \frac{0.203}{\alpha_s^2 \ln(0.580/\alpha_s)} \frac{1}{T} \quad \eta = \frac{0.344}{\alpha_s^2 \ln(0.608/\alpha_s)} T^3 \quad (9.57)$$

while for two flavors they are

$$D = \frac{0.165}{\alpha_s^2 \ln(0.497/\alpha_s)} \frac{1}{T} \quad \eta = \frac{1.095}{\alpha_s^2 \ln(0.521/\alpha_s)} T^3 \quad (9.58)$$

and for three flavors of massless quarks they are

$$D = \frac{0.150}{\alpha_s^2 \ln(0.461/\alpha_s)} \frac{1}{T} \quad \eta = \frac{1.351}{\alpha_s^2 \ln(0.464/\alpha_s)} T^3 \quad (9.59)$$

Here D refers to quark flavor diffusion. These QCD expressions have an extra logarithmic factor arising from the Debye screening of the long-range color Coulomb force.

9.7 Exercises

- 9.1 Derive (9.6) and (9.10).
- 9.2 Obtain the polarization tensor for QED in the HTL limit, starting with the effective Lagrangian of (9.33)–(9.35).
- 9.3 Derive the formulae for the spectral densities in (9.39).
- 9.4 Derive the formulae for gluon spectral densities that are analogous to those for quarks.
- 9.5 Verify that (9.44) satisfies (9.43).
- 9.6 Obtain the polarization tensor for QED in the HTL limit starting with (9.47).

References

1. Pisarski, R. D., *Nucl. Phys.* **B309**, 476 (1988); *Phys. Rev. Lett.* **63**, 1129 (1989).
2. Braaten, E., and Pisarski, R. D., *Nucl. Phys.* **B337**, 569 (1990).
3. Kalashnikov, O. K., and Klimov, V. V., *Yad. Phys.* **31**, 1357 (1980) (*Sov. J. Nucl. Phys.* **31**, 699 (1980)); *Phys. Lett.* **B88**, 328 (1979).
4. Weldon, H. A., *Phys. Rev. D* **26**, 1394 (1982).
5. Braaten, E., and Pisarski, R. D., *Phys. Rev. D* **45**, 1827 (1992).
6. Wong, S. K., *Nuovo Cimento* **65A**, 689 (1970).
7. Kelly, P. F., Liu, Q., Lucchesi, C., and Manuel, C., *Phys. Rev. D*, **50** 4209 (1994).
8. Taylor, J. C., and Wong, S. M. H., *Nucl. Phys.* **B346**, 115 (1990).
9. Blaizot, J.-P., and Iancu, E., *Phys. Rep.* **359**, 355 (2002).
10. De Witt, B. S., *Phys. Rev.* **162**, 1195, 1239 (1967).
11. Arnold, P., Moore, G. D., and Yaffe, L. G., *JHEP* **05**, 051 (2003).